



CERN LIBRARIES, GENEVA



SC00000159

CERN-DRDC 93-5

PROPOSAL P48

8/ 1/ 93

SCP
CERN-DRDC
93-5

PROPOSAL FOR PS BEAM TESTS OF A FAST RICH DETECTOR

J.Seguino*, J.P.Jobez and T.Ypsilantis*

College de France, Paris, France

E.Chesi

CERN, Geneva, Switzerland.

R.Arnold and J.L.Guyonnet

CRN, Strasbourg, France

J.Egger and K.Gabathuler

PSI, Villigen, Switzerland

M.French and M. Lovell

RAL, Abdingdon, United Kingdom

C. Joram, W. Kluge

University of Karlsruhe, Karlsruhe, Germany

I. Adachi, R. Enomoto, T. Sumiyoshi

KEK Laboratory, Tsukuba, Japan

Summary

A full scale prototype Fast RICH detector system with pad readout for unambiguous imaging has been constructed for operation in a high luminosity environment. It uses the best photosensitive gas capable of fast response (TEA) or the intrinsically fast solid photocathode (CsI/TMAE), developed specifically for this purpose. It can be used at e^+e^- or hadron colliders as well as at fixed target facilities. It has time resolution of 20 ns with a 1.3 μ s pipeline and parallel readout of 4000 pad sectors in 2-3 μ s. Fast digital VLSI electronics has been developed for readout and 24000 channels have been received and tested. The prototype device, with 12000 pad channels, is assembled and ready. Cosmic ray images, observed since December 1992, show that the counter and readout system work as expected. We therefore request PS test beam time during 1993.

A detailed experimental investigation has been made of a multiwire photon counter with TEA as the photosensor. We have also shown that this same counter works equally well with a CSI/TMAE reflective photocathode. These tests allowed optimization of the fast RICH construction parameters to fulfill the requirements of speed ($\sigma_t \approx 10-20$ ns), cathode pad detection efficiency ($\epsilon_c > 0.98$) and pixel resolution ($\sigma_x, \sigma_y \approx 1$ mm) over the full counter surface.

* CO-SPOKESMEN

1. INTRODUCTION

The limits of the ring imaging Cherenkov (RICH) technique for (π/K) particle identification (PI) can extend up to 230 GeV/c for gas radiators of about 1 m length [1]. This detector also gives ($e/\mu/\pi$) identification up to about 50 GeV/c and (K, P) identification to 400 GeV/c, as shown in fig. 1. These upper limits are determined by the optical dispersion of the best radiators (He, Ne, CF₄) in the energy response region (6 to 7 eV) of the best photoionizing gas (TMAE). In order to obtain fast response ($\sigma_t \approx 10$ ns) the photosensitive gas must have sufficient vapor pressure (20 to 50 Torr) however, this is not always possible at 20⁰ C. The photosensitive thin film CsI/TMAE is an excellent alternative because the photoelectrons are isochronous and drift times to the amplifying wires are short. Such a counter, with cathode pads and amplifying wires, is shown in fig. 2. It was originally designed to operate with the highly absorbing photosensitive gas TEA (in methane). It has an absorption mean free path of 500 μm (at 14⁰ C) and a drift velocity of 50 $\mu\text{m}/\text{ns}$ hence time dispersion $\sigma_t = 10$ ns, suitable for fast operation. A small test counter has been built and its anode and cathode response to single electrons has been measured [2]. The cathode pad efficiency exceeds 97% and the counter is stable for gains up to $2 \cdot 10^6$. Its only drawback is that the TEA photon response region lies between 7.5 and 8.9 eV (165 to 140 nm), where radiator media are more dispersive. In addition, operation in this region requires expensive and fragile single crystal windows (e.g. CaF₂) rather than inexpensive and robust fused quartz.

The photosensitive gas, TMAE, has good quantum yield in the 6 to 7 eV region but long absorption length (29 mm at 20⁰ C). In order to obtain the requested fast response ($\sigma_t = 10$ ns) this detector would need to operate above 100⁰ C. For these reasons we investigated solid thin film reflective photocathodes-vacuum deposited directly onto the cathode pads (see fig. 2). The quantum yield of reflective cathodes is always superior to transmissive cathodes because photoelectrons are produced with largest probability near the entrance surface which, in the reflective mode, is also the exit surface.

A report on the intrinsic resolution of RICH detectors [1] is appended to this proposal (Add 1).

2. THE PROTOTYPE FAST RICH COUNTER

This full scale Fast RICH counter is of the proximity focusing type with a crystal radiator (10 mm CaF₂ or LiF) followed by the lever-arm region (130 mm) and the detector structure (10 mm) and electronics (34 mm). It was originally designed as the RICH counter for the 4π detector at the late and lamented PSI e^+e^- collider B-Factory. It has a cylindrical radius extending from 650 to 850 mm with polygonal barrel staves of 900 mm half-length each subtending an azimuthal angle of 12⁰. Three barrel

sectors are constructed with cathode area of $\approx 0.4 \text{ m}^2$ divided into 12000 pads, each equipped with VLSI detection and readout electronics (see fig. 3). The asymmetric, 3 mm thick MWPC photon counter has its outer cathode surface made of rectangular metal pads ($5.3 \times 6.6 \text{ mm}^2$) which are read out individually to define image points. The pad size ($\Delta x, \Delta y$) is chosen so that the contribution to the total Cherenkov angle error σ_θ from the detection point (x, y) error is much less than the emission point (z_e) error due to radiator thickness [1], i.e. $\sigma_\theta(x) < \sigma_\theta(z_e)$ and $\sigma_\theta(y) < \sigma_\theta(z_e)$.

The CaF_2 windows are glued to the support structure so that counters can be replaced without disturbing the gas quality in the lever-arm region. This support structure provides the necessary mechanical rigidity and houses the gas inlets and outlets. Gold-plated tungsten anode wires (15 μm diameter) are strung with 1.27 mm pitch along the beam direction (y). They are supported at 110 mm intervals (in y) by ceramic spacers (0.5 mm thick) to fix the anode-cathode spacing and to minimize deflection due to electrostatic forces, thus ensuring more uniform gas gain. Conductive aluminum traces 100 μm wide are vacuum deposited on the inner surface of the CaF_2 window with pitch of 1.5 mm (along x) hence are 93% transparent. The electrostatic drift field of the MWPC cell is defined by the trace potential $U_w \approx -1.4 \text{ kV}$ with the anode wires at $U_a \approx 1.4 \text{ kV}$ and the pads at $U_k = 0$.

The rear stesalite plate of the photodetector supports the cathode pads and houses a ground plane through which pass the pad connections to the electronics. This ground plane acts both as an electrostatic shield and as the ground reference for the pad electronics ($U_k = 0$). The VLSI readout electronics are mounted on multilayer printed circuit boards contained inside a 34 mm deep aluminum tray-like structure.

Cherenkov photons, produced when a charged particle ($\gamma \geq 1.4$) passes through the radiator crystal, propagate through the transparent lever-arm region (N_2 filled) and are absorbed in the photodetector. The detected photoelectrons form a parabola-like image (not a ring) containing 10-20 points. The radiator thickness (10 mm) is fixed by the required number of image points and the lever arm distance (130 mm) by the needed angular resolution σ_θ .

Initially, we will operate with a mixture of methane saturated with TEA at 14°C ($p \approx 40 \text{ Torr}$, $l_{ph} \approx 0.5 \text{ mm}$) with a 3.5 mm thick CaF_2 entrance window. The total gas thickness (3 mm) absorbs 99.8% of the UV photons resulting in dispersion of the photoelectron arrival times ($\sigma_t \approx 10 \text{ ns}$) which allows reasonably fast data sampling (gate width $\geq 20 \text{ ns}$). The thinness of the gas layer greatly reduces the charged particle ionization signal and the resultant production of feedback photoelectrons. A fast wire signal can discriminate (by pulse height) between charged particles and photoelectrons and allow, for example, a secondary particle multiplicity trigger.

The proximity focusing method, used with crystal or liquid radiators, assures particle ID in the low momentum region (see fig. 1). The counter may operate either with a fast photosensitive gas (TEA) or with a fast reflective photocathode (CsI/TMAE). In the TEA response region (7.5 to 8.9 eV), chromatic dispersion of CaF_2

is large ($dn/dE=0.07 \text{ eV}^{-1}$) and limits the π/K separation to $3 \text{ GeV}/c$ (3σ) whereas the less dispersive crystal LiF ($dn/dE=0.031 \text{ eV}^{-1}$) allows π/K separation to $4 \text{ GeV}/c$. In the CsI/TMAE response region (6 to 7 eV), the π/K separation limit with the (CaF₂, LiF) radiator rises to (4.5, 5.0) GeV/c , respectively. A liquid C₆F₁₄ radiator with the CsI/TMAE response can separate π/K up to $7 \text{ GeV}/c$. This same counter, with $3 \times 3 \text{ mm}^2$ pads, can detect mirror focused-gas radiator-images to assure particle ID in the high momentum region (see fig. 1).

The present TEA based counter with its CaF₂ entrance window, gas volume and electronics has a mass of $10\% X_0$ while the 10 mm thick CaF₂ radiator has $8.6\% X_0$ for a total $19\% X_0$. With a CsI/TMAE photocathode it may be possible to suppress the entrance window thus reducing the detector mass to about $6\% X_0$. In addition, the radiator will be replaced by the low Z crystal LiF ($7.5 \text{ mm}=5\% X_0$) to give the total counter mass $11\% X_0$. Minimizing this mass is important in an e^+e^- B-Factory, because the detector precedes a high precision EM calorimeter.

3. THE SMALL TEST COUNTER

A small Fast RICH test counter was constructed with an asymmetric MWPC operating with TEA as the photosensitive gas and with detection of an induced cathode pad signal. The gas thickness between the UV transparent window and the cathode pad surface is 2.5 mm which, for methane saturated with TEA at 20°C , represents 4.5 photon absorption lengths for $E=8.2 \text{ eV}$ photons. The cathode surface is segmented into 6×8 rectangular pads each of area $5.1 \times 7.6 \text{ mm}^2$. Each pad is linked to the outer surface of the detector by metal pins which connect to the preamplifier.

The distance (d) between the anode wire plane and the cathode pad surface is adjustable between 0.4 and 0.7 mm in order to measure the variation of the induced pad signal and determine its dependence on this parameter. Gold plated tungsten wires ($15 \mu\text{m}$ diameter) are strung parallel to the long pad dimension with a pitch of 1.27 mm. For $d \leq 0.5 \text{ mm}$ the induced pad signal is always sufficiently large to give high pad efficiency ($\geq 98\%$). The detector entrance window is a CaF₂ single crystal disk 76 mm in diameter and 5 mm thick. A resistive tungsten coating ($R=25 \text{ k}\Omega$, 1.5 nm thick) is vacuum deposited on the inner surface of the window to define the upper cathode potential. The transmittivity of this coating is 40% at 8.2 eV (unacceptable for a working RICH detector but acceptable for these tests since more than enough light intensity is available from the flash lamp to compensate this loss). The window transmittivity is consequently uniform over the surface, as required to test the intrinsic position sensitivity of the detector. A thermostatically stabilized bubbler is used to saturate the carrier gas with TEA (or TMAE). The carrier gas with TEA is pure methane and with TMAE is a mixture of 75% methane with 25% isobutane.

A full report of these tests and resolution measurements are contained in reference [2] which is appended (Add 2) to this proposal.

4. THE CsI+TMAE ADSORBED FILM REFLECTIVE PHOTOCATHODE

A CsI reflective photocathode, vacuum deposited on a metal substrate, adsorbs a thin layer of TMAE when a low concentration of TMAE gas is flowed (for about 1 hour) over the the CsI surface. Such a sensitized photocathode has an extremely high quantum efficiency (46% at 175nm) and can operate in the reflective mode with the pad counter of fig. 2. Our developmental work on CsI and CsI/TMAE reflective photocathodes [3] is appended to this proposal (Add. 3).

The Cherenkov response parameter $N_0=(370 \text{ eV}^{-1}\text{cm}^{-1})\cdot\epsilon\cdot\Delta E$ where ΔE is the energy bandwidth of the counter and ϵ the energy averaged detection efficiency (quantum, mirror reflection and window transmission). Taking the experimental values 0.8 for reflection, 0.8 for transmission and an average quantum efficiency of 27.5% (i.e. 12% at 6 eV and 43% at 7 eV) we expect $\epsilon=.176$ for $\Delta E=1 \text{ eV}$ hence, a response parameter $N_0=65 \text{ cm}^{-1}$. This is exactly the response parameter and energy bandwidth used in [1] to calculate the particle identification capability shown in fig. 1. Thus, we see that this photocathode has good sensitivity, moreover, it can operate in the less dispersive energy range compatible with fused quartz windows.

The advantages of a CsI/TMAE photocathode are speed, high efficiency and simplicity but its disadvantages are yet to be known. Photon feedback will probably be the biggest problem in a counter with gaseous amplification. Gas phase feedback, however, cannot occur because the TMAE partial pressure is negligible. Feedback from the cathode itself will tend to merge with the primary avalanche if (as is the case here) the amplifying wire is near the cathode (i.e. 0.5 mm=10 ns). To minimize feedback, the amplifying gas should be opaque to the C* lines at 156 and 166 nm (i.e. 7.95 and 7.47 eV). Isobutane (in methane) serves this purpose as well as defining the upper energy of response (e.g. 7.1 eV). The C* emission line at 193 nm (6.42 eV) is then the only remaining source of feedback instability. The level of photon feedback is expected to be equal to that of a TEA based gas counter which is sensitive only to the 156 nm emission line. This is because the feedback probabilities of the 156 and 193 nm lines are equal, as are the corresponding TEA and CsI/TMAE quantum efficiencies. Tests of the small TEA counter have shown enhanced stability to photon feedback compared to a TMAE counter, even for gains up to $2\cdot 10^6$ [2].

We have also tested a small pad counter (identical to that in section 3) with vacuum deposited CsI or CsI/TMAE reflective photocathodes [4] and this report is appended to this proposal (Add. 4). These data confirm the expected fast and stable single photon response but with a quantum efficiency only $\approx 50\%$ of the expected value. This loss is attributed to a long air exposure while stringing the wires (after the cathode was deposited). For the Fast RICH prototype the wires will be attached to the window frame (independent of the cathode) thus allowing fast assembly with minimum air exposure of the cathode.

5. DEVELOPMENT OF THE PAD READOUT VLSI ELECTRONICS

We have developed and measured the performance of the analog and digital VLSI readout electronics as given in [5] and appended to this proposal (Add. 5). Since all RICH detector applications envisioned have $\geq 10^5$ pads, the need for VLSI electronics is obvious. Detection, selection, memorization and readout are performed in situ so that connections to the data acquisition system (DAQ) are limited to 5 data monitoring and 6 bus lines per 12^0 half-sector of 4000 channels. The two VLSI chips were developed at the microelectronics division of the Rutherford Laboratory. The chip production costs are 3.7 SF per channel (which rises to 6.2 SF/channel when the chips are mounted and interfaced to the DAQ system). Chip development costs are not included in these figures.

5.1 BIPOLAR CHIP: ANALOGUE PREAMPLIFIER AND PIPELINE

This 8 channel analog chip, developed in bi-polar technology, contains a current preamplifier, amplifier and discriminator. The mean rms noise level at the input is 625 electrons (10 nA noise current in RC response time of 10 ns). The chip discriminator threshold is adjustable (for all 8 channels of the chip) between 1 and 16 (modulo 625 e) by a 4-bit address supplied by the DAQ system.

5.2 CMOS CHIP: FAST DIGITAL READOUT WITH ZERO SUPPRESSION

This 16 channel digital chip developed in CMOS technology has a $1.32 \mu\text{s}$ delay pipeline at the input realized by a 64 step shift register operating at 50 MHz. Its purpose is to provide the time delay for a first level trigger. The delayed trigger pulse is used to generate a write gate (≥ 20 ns wide) which selects the corresponding RICH event. The readout circuit proper is integrated on this same CMOS digital chip. Each channel has an input register and each chip contains a 4-bit priority encoder to suppress zeroes and provide the address of the hit pad. The data are loaded into a 16 word RAM and then shifted along the pad column at a frequency of 20 MHz. At the start of a read sequence, the shift logic compacts the data upward (to the top of each column) thus minimizing the clock pulses needed for data extraction. Each column is then readout sequentially, giving the hit pad row address and the column address. Measurements show that the average readout time $t_{ro} = (1.5 + 0.05N_h) \mu\text{s}$, where N_h is the expected number of pad hits per sector (10-20 for a full image). The total readout time will therefore be several microseconds, with parallel readout of the other 4000 channel sectors.

6. DATA ACQUISITION SYSTEM

Routing of the data flow is broken up into a data part and the control part. Each of these is composed of an emitter and a receiver located either close to the detector or in the VME crate. The data interface is fast (20 MHz) but the control interface is slow (100 kHz).

6.1 THE DATA INTERFACE

The emitter is near the detector and has as input the CMOS encoded signals from 4000 pads of a sector. The emitter output (ECL level) is a 32 bit word containing the address of the hit pad (row, column) and other fixed data (i.e. event id, run id, event separator).

The receiver is a dual ported RAM which is plugged into the VME bus. It's size is 64k organized in 32 bit words when accessed from the external port. On the VME side, the RAM is read/write accessible in 1, 2 or 4 bytes. The first 32 bits of the RAM is a 16 bit counter indicating the number of written words from the external port. This counter is reset at its location by the read cycle. The maximum rate on the external port is 30 MHz. Transfer is synchronized by a clock in single ECL level.

6.2 THE CONTROL INTERFACE

The emitter (ELTEC), plugged into the VME bus, has a programmable interface with 48 I/O with TTL drivers, 4 of these are used in the DAQ system as interruption inputs to the processor. The receiver is located close to the detector and controls the operation mode of a sector (test, threshold, acquisition) according to the emitter (threshold values and test data).

6.3 THE DATA ACQUISITION SYSTEM OS-9

The main features of this system are the following:

- 68030 microprocessor operating at 25 MHz

- 8 Mbytes RAM

- Ethernet interface

- 135 Mbytes hard disk

- 120 Mbytes tape streamer

The data acquisition system is organized around an on-line "task" (data producer), an interrupt routine, and several low priority tasks (data consumer). When in execution, the data producer cannot be halted by the real-time kernel.

Once signal interruption occurs the interrupt routine disables the trigger system by means of a veto and copies the content of the data receiver boards into the RAM

of the OS9. The interrupt routine then releases the veto and sends an wake-up signal to the data producer. Task gathers the data of the same event received in different data receivers and writes them into another data module called EVENT. Task then goes back to sleep until the next interrupt signal.

The data in the EVENT data module are available to data consumers such as "monitoring task" or "storage task". The write permission in the EVENT data module is only given to the data producer and read/write pointers are used to control the access to this data module so as to avoid overwriting.

7. FUNDING, SCHEDULE, OUTLOOK AND NEW COLLABORATORS

This project was started in 1988 and is now essentially complete. The funding profile is shown in Table 1. The actual costs for the Fast RICH prototype fabrication are listed in Table 2.

As cosmic ray tests have shown that the TEA based counter and electronics work as expected, we are ready for PS beam tests starting spring 1993. In a later phase (summer 1993) we will replace the TEA based with a CsI/TMAE based detector.

Because the counter is sufficiently fast and the electronics sufficiently performant, we believe that this detector system will satisfy the needs of collider (and fixed target) B experiments at LHC.

We are constructing, with our Japanese collaborators, an identical Fast RICH prototype detector with the same electronics for later tests at KEK. Their goal is to be ready for a KEK B-Factory which will probably be approved for construction in 1994.

In the future we will be joined by a group from Syracuse University who are interested in a RICH particle identifier for the CLEO detector upgrade. The new collaborators are M. Artuso, M. Goldberg, G. Monetti and S. Stone.

TABLE 1
FAST RICH FUNDING (kSF), (1SF=4FF)

<u>YEAR</u>	<u>IN2P3 = CdF + Stras</u>	<u>CERN</u>				
		<u>PSI</u>	<u>LAA</u>	<u>KEK</u>		
1988	100=	62.5	37.5			
1989	125=	75	50			
1990	187=	137	50			
1991	105=	50	25			
1992	96=	55	41			
1993	50	Pending				
Sub Totals	613=	409.5	203.5	170	150	125
Total						1058

Fast RICH Prototype **Funding** = 1058 - (88/89 CdF)* - (Stras)** = 716.5

Fast RICH Prototype **Cost** (see TABLE 2) = 686.1

Reminder: to be used for beam tests = 30.4

* The 1988/89 CdF funding was used mainly for tests of the small TEA photodetector and development of the CsI and CsI/TMAE photocathodes (charge collection only). These photocathodes, of course, will be used in the 2nd phase of the beam tests.

** Mostly for tests with the small TEA photodetector and tests of a CsI photocathode single photoelectron counter (with gas amplification). In addition, modification of our beam MWPCs, to use the new VLSI readout electronics, was largely done at Strasbourg and Karlsruhe.

TABLE 2
FAST RICH PROTOTYPE COSTS (kSF)

<u>ITEM</u>	<u>CdF</u>	<u>PSI</u>	<u>CERN</u>		<u>STATUS</u>
			<u>LAA</u>	<u>K'RUHE</u>	
Frame Mechanics	87.5				Paid
Pad Development	19.3				Paid
Pad Production	23.2				Paid
Pad Plane Cabling	5.5				Paid
Data Acquisition			41.0		Paid
Chip Development	165.0		47.8		Paid
Chip Production	53.0		41.0		Paid
Radiators CaF ₂		13.8			Paid
Radiators LiF		10.6			Paid
Windows CaF ₂		35.4			Paid
Window Trace Deposits				Done	Paid
Test Beam Table		5.0			Paid
Manpower		54.0			Paid
PCB's 3 Sectors			15.0		Paid
Cabling 3 Sectors	10.0				Paid
Components 3 Sectors	11.0				Paid
Electronician		48.0			Paid
Sub Totals	374.5	166.8	144.8		
Total					686.1

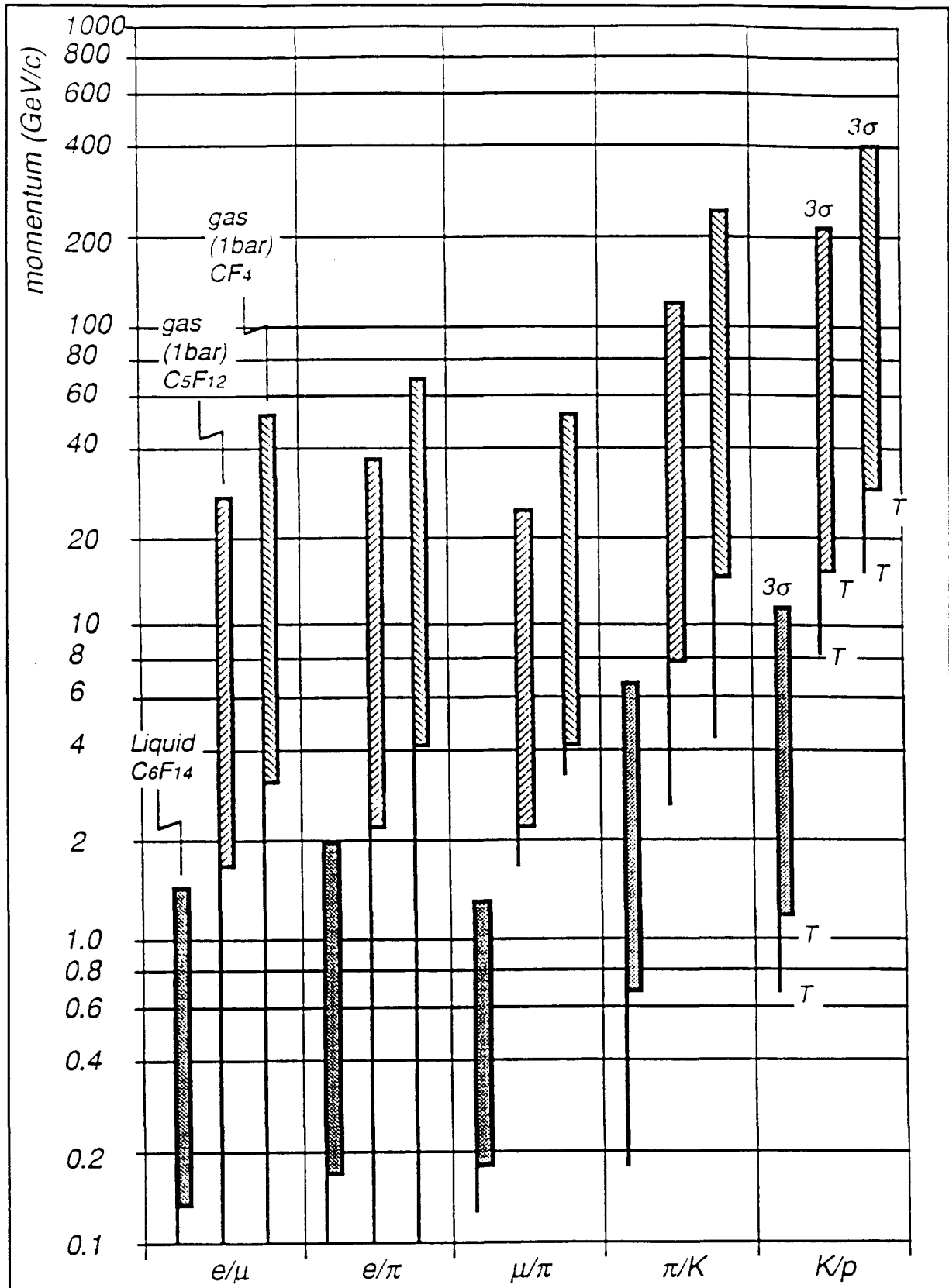


Fig. 1. Particle ID chromatic limits (6 to 7 eV, $N_0=65 \text{ cm}^{-1}$) for three radiators: 1 cm liquid C_6F_{14} proximity focused with 0.2 m lever-arm; 40 cm C_5F_{12} gas mirror focused ($f=1.8 \text{ m}$); 140 cm CF_4 gas, mirror focused ($f=1.8 \text{ m}$). Particle ID is by threshold for the regions with thin lines, by RICH for the boxed regions. Top limits are 3 s.d. and T indicates threshold.

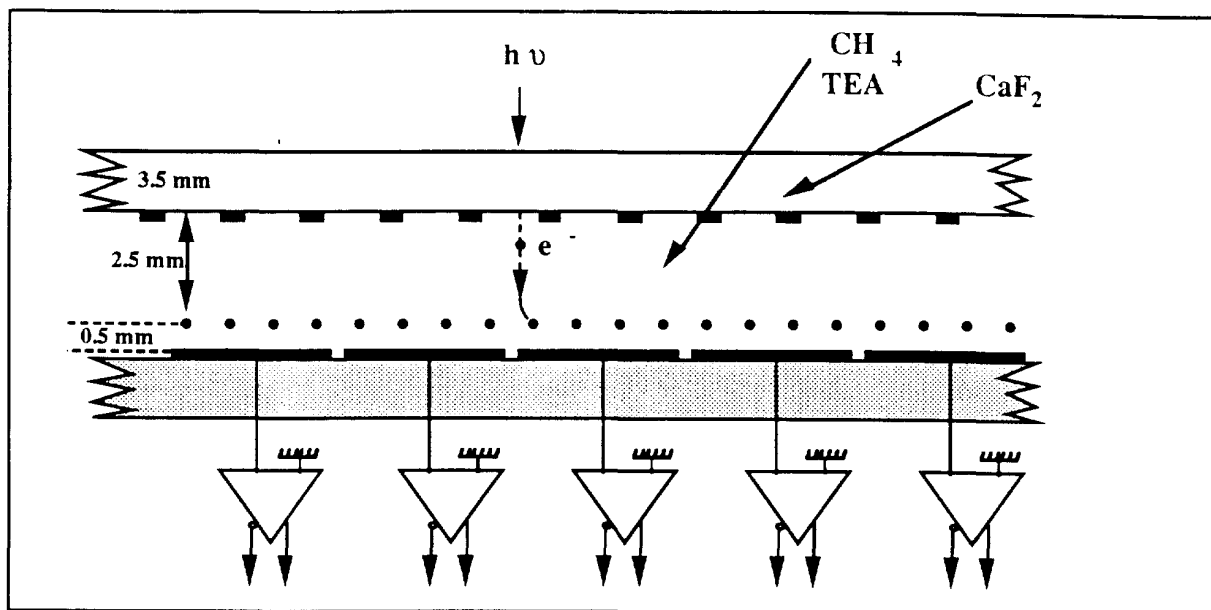


Fig. 2. The Fast RICH detector geometry

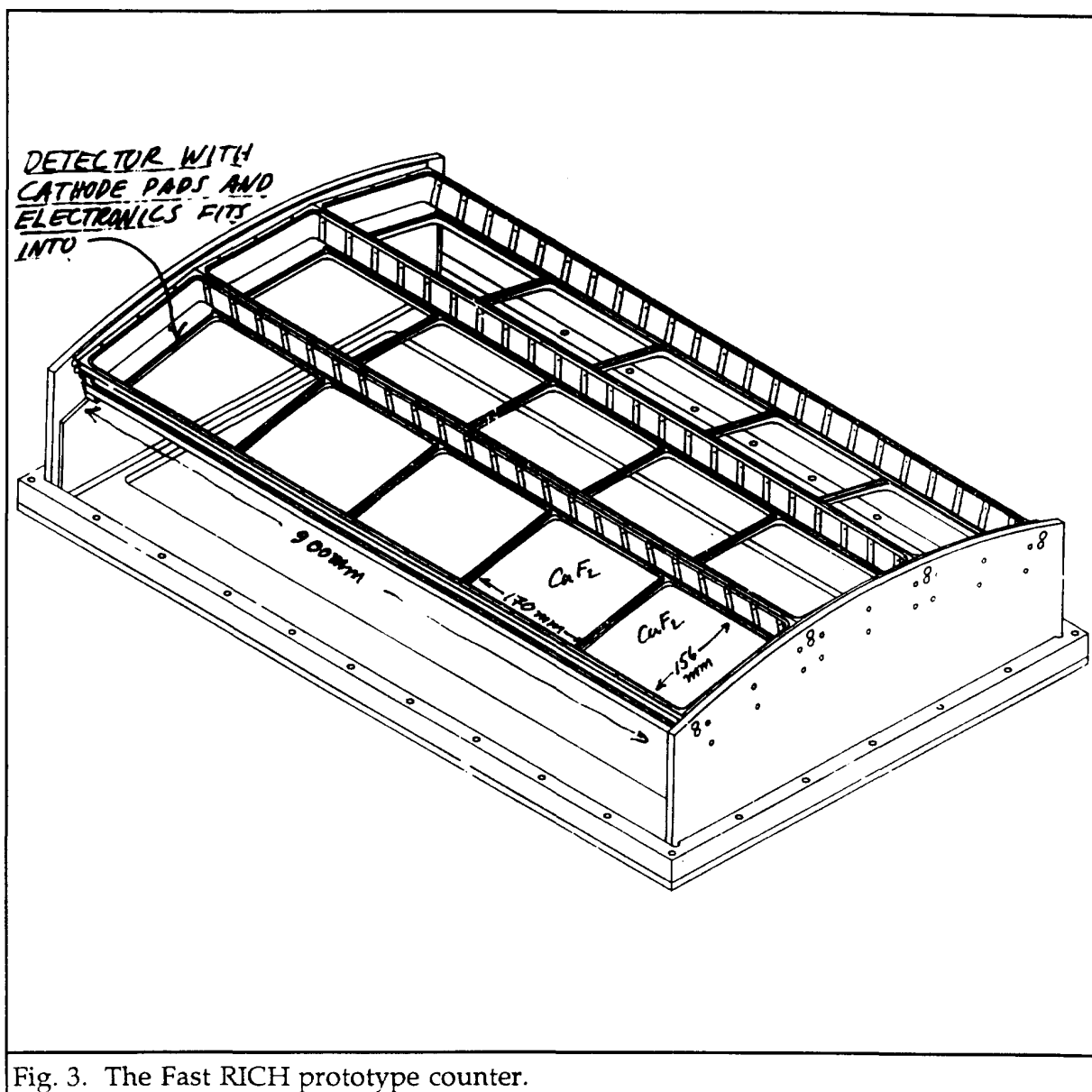


Fig. 3. The Fast RICH prototype counter.

REFERENCES

[1] T.Ypsilantis. CERN-EP 89-150

[2] R.Arnold, Y.Giomataris, J.L.Guyonnet, A. Racz, J.Seguino and T.Ypsilantis. Nucl. Instr. and Meth. A314 (1992) 465.

[3] J.Seguino, G.Charpak, Y.Giomataris, V.Peskov, J.Tischhauser and T.Ypsilantis. Nucl. Instr. and Meth. A297 (1990) 133.

[4] R. Arnold, E. Christophel and J.L. Guyonnet. CRN/HE 91-06.

[5] M. French, M. Lovell, E. Chesi, A. Racz, J.Seguino, T.Ypsilantis, R. Arnold, J.L. Guyonnet, J. Egger and K. Gabathuler. CERN/ECP 92-2 and NIM in press.